Catal Lett (2007) 118:195–202
DOI 10.1007/s10562-007-9160-3

Impact of Boron Modification on MCM-41-Supported Cobalt Catalysts for Hydrogenation of Carbon Monoxide

Pimchanok Tupabut · Bunjerd Jongsomjit · Piyasan Praserthdam

Received: 15 May 2007 / Accepted: 5 June 2007 / Published online: 23 June 2007

Abstract Boron modification on MCM-41-supported cobalt (Co) catalysts was found to decrease the catalyst activity during CO hydrogenation. The decreased activities were due to stronger support interaction between Co oxide species and the support with the presence of boron resulting in lower reducibility. However, based on methanation the selectivity to C_2–C_4 products slightly increased with low loading of boron.

Keywords Cobalt catalyst · MCM-41 · Support · Boron modification · CO hydrogenation

1 Introduction

For years, supported cobalt (Co) catalysts are the preferred catalysts for Fischer-Tropsch synthesis (FTS) because of their high activity during FTS based on natural gas [1], high selectivity for linear long chain hydrocarbons and low activity for the competitive water-gas shift (WGS) reaction [2, 3]. It has been known that activities of the Co catalysts apparently depend on the number of reduced Co metal atoms dispersed on the support used, thus the nature of support can play important roles on such the phenomenon. Many inorganic supports such as silica (SiO_2) [4–8], alumina (Al_2O_3) [9–11], and titania (TiO_2) [12–16] have been extensively studied as catalytic support materials for Co catalysts for years. It is known that in general, the catalytic properties depend on reaction conditions, catalyst composition, metal dispersion, and types of inorganic supports used. Thus, changes the catalyst compositions and/or even though the compositions of supports used could lead to a significant enhancement of the catalytic properties as well. It was mentioned that some support modifiers such as boron (B) and zirconia (Zr) showed the promising enhancement of catalytic activities for some supports such as Al_2O_3 [11] and TiO_2 [16].

Recently, there have been a considerable number of papers and reviews dealing with the synthesis and characterization of highly uniform mesoporous materials, particularly the hexagonal pore silica-based MCM-41 [17, 18]. The MCM-41 usually has a very high BET surface area, ca. 1000 m^2/g, uniform pore size with average pore dimensions between 1.5 and 10 nm, and high thermal and hydrothermal stability. Use of MCM-41 as a metal catalyst support has resulted in several cases in significant improvements compared to conventional commercial catalysts due to superior dispersion of the active metals [19–21].

In this present study, the impact of boron modification on MCM-41-supported cobalt catalysts for hydrogenation of CO was investigated. The amounts of boron added onto the MCM-41 support were varied. The cobalt precursor was deposited onto the modified support by the incipient wetness impregnation method. After calcination, the catalyst samples were characterized by means of XRD, SEM/EDX, TEM, TPR, Raman spectroscopy, and XPS. Then, they were tested for activity and selectivity towards CO hydrogenation. For a comparative study, the boron modification onto SiO_2-supported cobalt catalysts was also conducted.

P. Tupabut · B. Jongsomjit (✉) · P. Praserthdam
Department of Chemical Engineering, Faculty of Engineering, Center of Excellence on Catalysis and Catalytic Reaction Engineering, Chulalongkorn University, Bangkok 10330, Thailand
e-mail: bunjerd.j@chula.ac.th

2 Experimental

2.1 Catalyst Preparation

The MCM-41 support was synthesized according to the method described by Panpranot et al. [22] using the gel composition of CTABr: $0.3NH_3$: $4SiO_2$: Na_2O: $200H_2O$, where CTABr denotes cetyltrimethyl ammonium bromide. Briefly, 20.03 g of colloidal silica Ludox HS 40% (Aldrich Chemical Company, Inc.) was mixed with 22.67 g of 11.78% sodium hydroxide solution. Another mixture comprised of 12.15 g of CTABr (Aldrich Chemical Company, Inc.) in 36.45 g of deionized water, and 0.4 g of an aqueous solution of 25% NH_3. Both of this mixture was stirred by agitator for 30 min, then heated statically at 100 °C for 5 days. The obtained solid material was filtered, washed with deionized water until no base was detected and then dried at 100 °C. The sample was then calcined in flowing nitrogen up to 550 °C (1–2 °C/min), then in air at the same temperature for 5 h.

The boron-modified MCM-41 supports having 1, 3, and 5 wt.% of boron were prepared by the incipient wetness impregnation using boric acid as the boron source. The modified supports were dried overnight at 110 °C and then calcined in air at 500 °C for 4 h. The various MCM-41 supports with different amounts of boron modification were then impregnated with an aqueous solution of $Co(NO_3)_2 \cdot 6H_2O$ (Aldrich) by the incipient wetness impregnation in order to obtain the final catalyst having 20 wt.% of Co. The catalyst precursors were dried at 110 °C overnight and then calcined in air at 500 °C for 4 h. For a comparative study, the identical procedure was applied using the amorphous SiO_2 from Strem chemicals instead of the MCM-41 support.

2.2 Catalyst Nomenclature

The nomenclature used for the supports and catalyst samples in this study is as follows:

MB-*i*: the boron-modified MCM-41 having *i* wt.% of boron
SiB-*i*: the boron-modified SiO_2 having *i* wt.% of boron
Co/MB-*i*: cobalt catalyst on the boron-modified MCM-41 having *i* wt.% of boron
Co/SiB-*i*: cobalt catalyst on the boron-modified SiO_2 having *i* wt.% of boron

2.3 Catalyst Characterization

2.3.1 BET Surface Area

The BET surface area, pore volume, average pore diameter, and pore size distribution of the catalysts were determined by N_2 physisorption using a Micromeritics ASAP 2010 automated system. Each sample was degassed in the Micromeritics ASAP 2010 at 10^{-6} mm Hg and 200 °C for 4 h prior to N_2 physisorption.

2.3.2 X-ray Diffraction

XRD was performed to determine the bulk crystalline phases of samples. It was conducted using a SIEMEN D-5000 X-ray diffractometer with CuK_α (λ = 1.54439 Å). The spectra were scanned at a rate of 2.4° min^{-1} in the range of 2θ = 10–80°.

2.3.3 Temperature-programmed Reduction

The reduction behaviors of the calcined cobalt catalysts were measured by temperature-programmed reduction. TPR of sample was performed with a temperature ramp of 10 °C/min from 30 to 800 °C in a flow of 5% H_2 in Ar. H_2 consumption was measured by analyzing the effluent gas with a thermal conductivity detector (TCD).

2.3.4 Scanning Electron Microscopy and Energy Dispersive X-ray Spectroscopy

Catalyst granule morphology and elemental distribution were obtained using a Hitachi S-3500N scanning electron microscopy (SEM). The SEM was operated using the back scattering electron (BSE) mode at 20 kV and a working distance (the distance between the sample and the electron beam) of 20 mm. After the SEM micrographs were taken, EDX was performed to determine the elemental concentration distribution on the catalyst granules using INCA software.

2.3.5 Transmission Electron Microscopy

The dispersion of cobalt oxide species on the various supports was determined using a JEOL-TEM 200CX transmission electron microscopy operated at 200 kV with 25 k magnification.

2.3.6 Raman Spectroscopy

The Raman spectra of the samples were collected by projecting a continuous wave YAG laser of Nd (810 nm) through the samples at room temperature. A scanning range of 100–1000 cm^{-1} with a resolution of 2 cm^{-1} was applied.

2.3.7 X-ray Photoelectron Spectroscopy

XPS was used to determine the binding energies (BE) and surface concentration of samples. It was carried out using

the Shimazu AMICUS with VISION 2-control software. The energy reference for Ag metal (368.0 eV for $3d_{5/2}$) was used for this study.

2.4 Reaction

CO hydrogenation (H_2/CO = 10/1) was performed to measure the overall activity of the samples. Hydrogenation of CO was carried out at 220 °C and 1 atm. A flow rate of H_2/CO/Ar = 20/2/8 cc/min in a fixed-bed flow reactor. A relatively high H_2/CO ratio was used to minimize deactivation due to carbon deposition during reaction. Typically, 20 mg of a sample was reduced in situ in flowing H_2 (30 cc/min) at 350 °C for 10 h prior to the reaction. Reactor effluent samples were taken at 1 h intervals and analyzed by GC. In all cases, steady-state was reached within 5 h.

3 Results and Discussion

This study focussed on the effect of boron (B) modification on MCM-41 and silica-supported cobalt catalysts for CO hydrogenation. It was found that the BET surface areas of MCM-41 and silica employed were 510 and 155 m^2/g, respectively. After B modification, the BET surface areas of B-modified MCM-41 supports were ranged between 414 and 355 m^2/g upon increased amounts of B loading. The BET surface areas of B-modified silica supports were ranged between 165 and 147 m^2/g with increasing the amounts of B loading. Based on BET surface area results, it can be observed that the modification of B (1–5 wt.% loading) apparently resulted in decreased surface areas for both MCM-41 and silica supports. In addition, it was observed that the B modification did not change the pore size distribution (not shown) for the silica and MCM-41 supports. In fact, the more amounts of B loading, the less surface areas of the supports obtained. The XRD patterns for silica supports with and without B modification are shown in Fig. 1. It can be observed that at 28°, the XRD peak of B_2O_3 can be detected. The intensity of the peak apparently increased with increasing the amounts of B loading. After impregnation, the modified silica with cobalt precursor, the catalyst samples were calcined and then characterized with various techniques. The XRD patterns of various Co/SiB catalysts are shown in Fig. 2. They all exhibited the XRD peaks at 31° (weak), 36° (strong), and 65° (weak), indicating Co_3O_4 species. The XRD patterns for MCM-41 supports with and without B modification and the Co/MB catalysts are shown in Figs. 3 and 4, respectively. In particular, the similar trend as mentioned for the silica supports was also observed for the MCM-41 supports with and without B modification. In order to study the

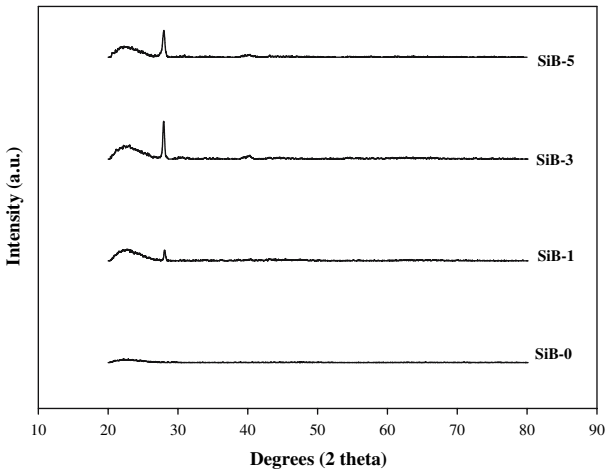

Fig. 1 XRD patterns for B-modified SiO_2 having various B loading

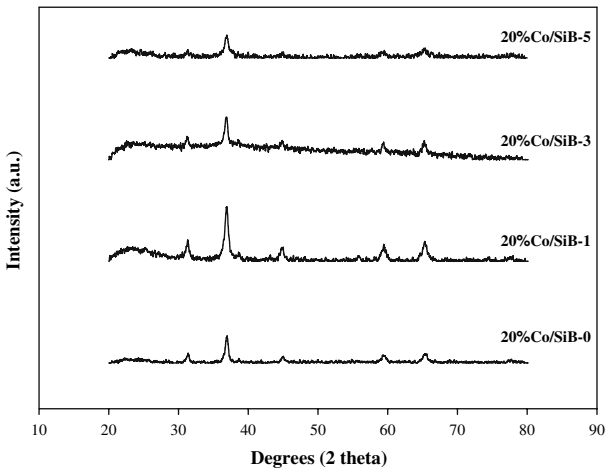

Fig. 2 XRD patterns for various 20%Co/SiB-i catalysts

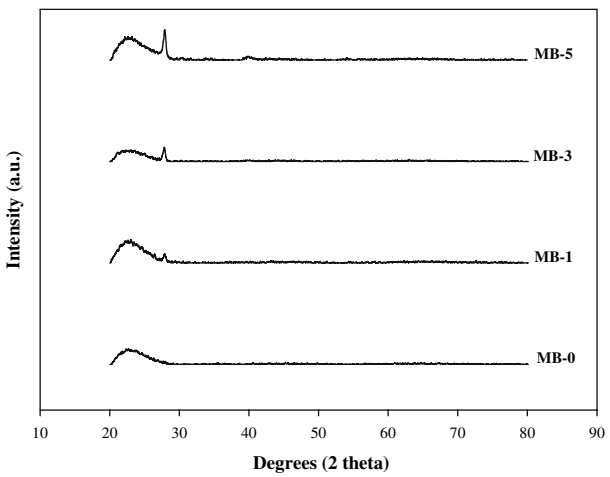

Fig. 3 XRD patterns for B-modified MCM-41 having various B loading

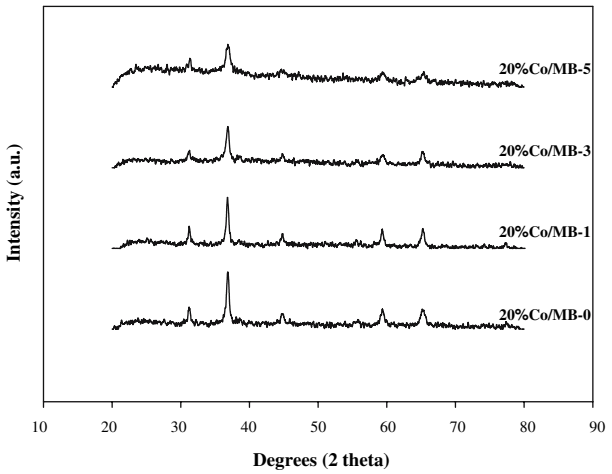

Fig. 4 XRD patterns for various 20% Co/MB-i catalysts

morphologies and elemental distribution of the catalyst samples, SEM and EDX were performed, respectively. The typical SEM micrographs and the elemental distribution for Co, Si, and O for Co supported on the silica support without B modification and with 3 wt.% of B modification are shown in Figs. 5 and 6, respectively. Based on the results of Raman spectroscopy (not shown), it was found that no significant Raman bands were observed for the supports without B modification between 200 and 1000 cm^{-1}. However, the Raman band for B_2O_3 was observed at ca. 880 cm^{-1} with B modification. The XPS profiles (not shown) for the typical B 1s exhibited the binding energy at 192.5–192.8 eV. It can be observed that all elements, especially Co oxide species exhibited good distribution all over the catalyst granule. There was no significant change upon the modification of silica with B. The typical SEM micrographs and EDX mapping for Co supported on the MCM-41 support without B modification and with 3 wt.% of B modification are also shown in Figs. 7 and 8, respectively. The similar trends as mentioned for Co supported on silica were observed indicating good distribution of Co oxide species all over the catalyst granule. In order to determine the dispersion and crystallite size of Co oxides species dispersed on the supports employed, the high resolution TEM was used. The TEM micrographs for Co oxides species dispersed on silica supports with and without B modification are shown in Fig. 9 whereas those for MCM-41 supports are shown in Fig. 10. As seen in both Figures, the dark sports represented the Co oxide species dispersed on the various supports. It can be seen from Fig. 9 that Co oxide species on the silica supports were well dispersed having the crystallite size of ca. 50–100 nm. Apparently, the crystallite size seemed to decrease with B modification. Similarly, the TEM micrographs as shown in Fig. 10 of Co oxide species on the MCM-41 supports were also well dispersed having the crystallite size of 100 to 200 nm. It can be seen that the crystallite size of Co oxide species on the silica supports was smaller than that on the MCM-41 supports indicating more agglomeration of Co oxide species.

As mentioned, TPR was performed in order to determine the reduction behaviors of Co oxides species on various samples. The TPR profiles of Co supported on silica supports with and without B modification are shown in Fig. 11. Basically, only two reduction peaks can be observed. The peaks can be assigned to the two-step reduction of Co_3O_4 to CoO and then to Co^0 [23, 24]. Upon the TPR conditions, the two reduction peaks based on two-step reduction may or may not be observed. The TPR profile of

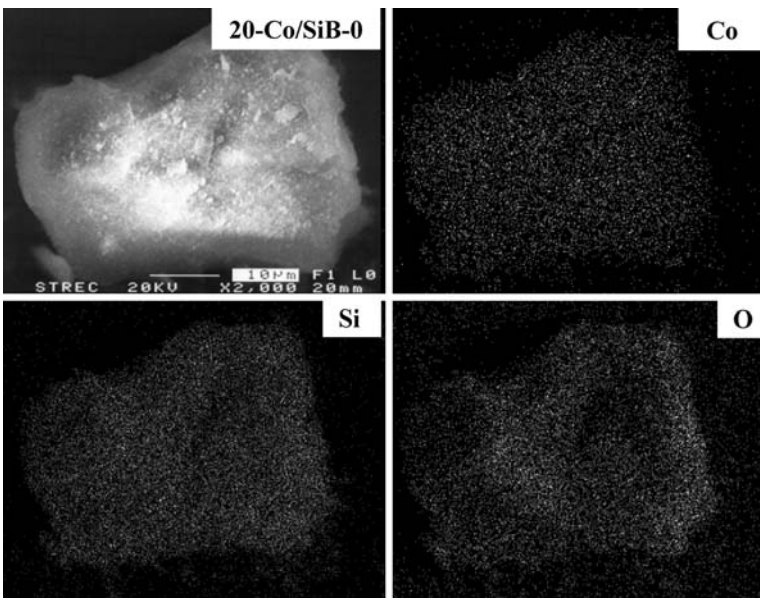

Fig. 5 A typical SEM micrograph and EDX mapping for 20-Co/SiO_2

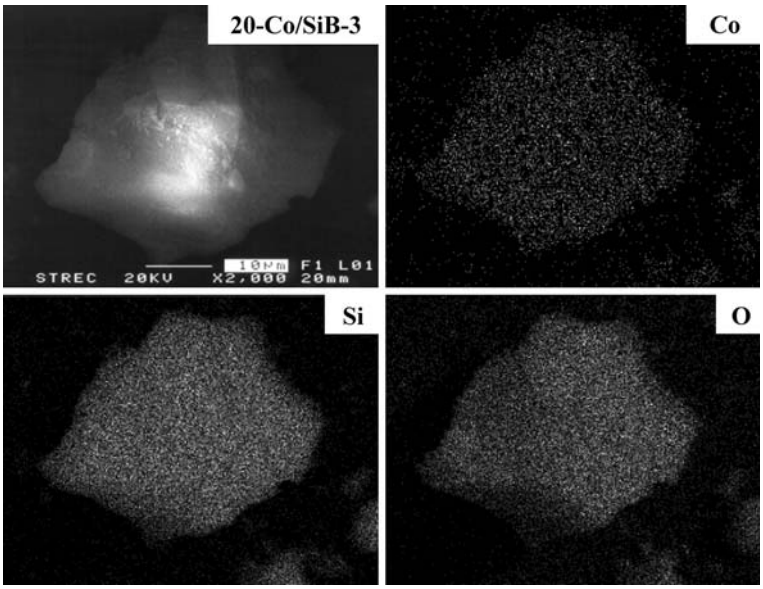

Fig. 6 A typical SEM micrograph and EDX mapping for 20-Co/SiO_2 with B modification

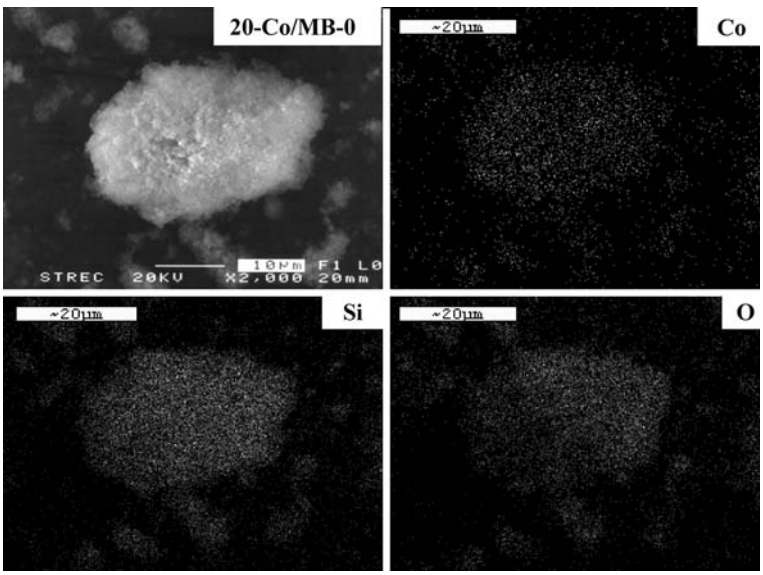

Fig. 7 A typical SEM micrograph and EDX mapping for 20-Co/MCM-41

the support with B modification showed no reduction peak. It appeared that the B modification resulted in higher degree of interaction between Co oxide species and the support indicating the shift of reduction temperature being higher with B modification. In addition, increased amounts of B modification caused in the increased degree of interaction between Co oxide species and the support. The TPR profiles of Co oxides supported on the MCM-41 with and without B modification are shown in Fig. 12. Apparently, the similar trend as mentioned for the silica supports was still observed. Essentially, B modification on silica and MCM-41 support resulted in higher degree of interaction, then being more difficult for such the Co oxide species to be reduced with the presence of B. However, when compared the reduction behaviors of Co supported on silica and MCM-41 supports. It seemed that the impact of B modification on the MCM-41 supports was more pronounced indicating the shift of reduction temperature to higher values. In fact, the effect of B source on the catalyst reducibility and Fischer-Tropsch synthesis activity of Co/TiO_2 catalysts was investigated by Coville et al. [25]. They reported that for all series of catalysts, at low B loadings (B wt.% < 0.05), reaction rates increased with increasing B loading; at high B loadings (B wt.% > 0.1%), there was a decrease in reaction rate. Li et al. [26] also reported that the addition of boron (0.05 wt.%) onto Co/TiO_2 did not

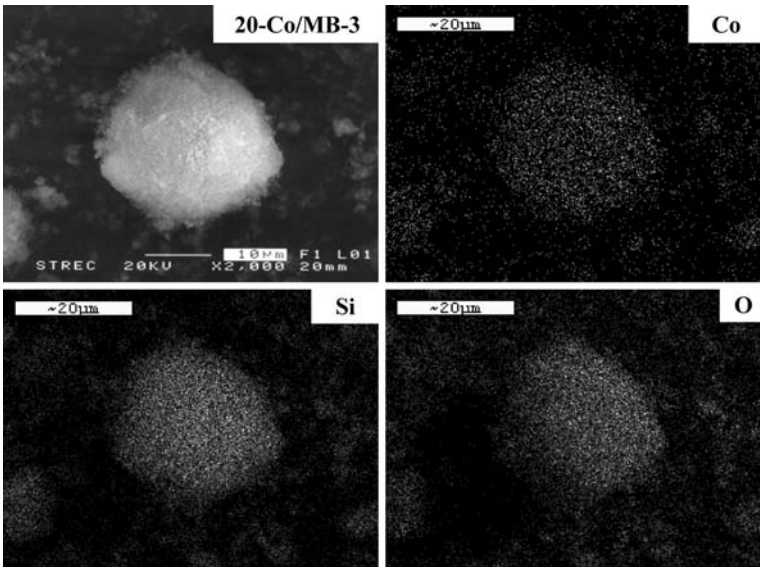

Fig. 8 A typical SEM micrograph and EDX mapping for 20-Co/MCM-41 with B modification

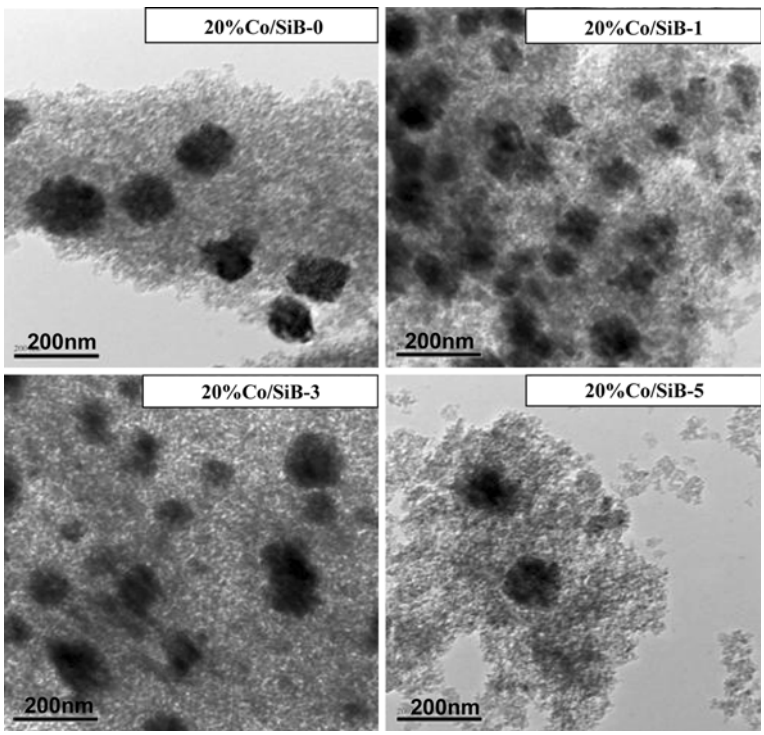

Fig. 9 TEM micrograph for 20-Co/SiO_2 with/without B modification

change the activity of the catalyst at lower space times and slightly increased the conversion at higher space times. The result [25] was in agreement with what we have found here regardless of the supports used. Thus, B modification consistently caused a decrease in reducibility of Co catalysts due to strong support interaction.

The reaction study under CO hydrogenation was also investigated in order to measure the activity and selectivity of catalysts. The reaction study results are listed in Table 1. It can be seen that for the silica supports, the modification of B resulted in lower activity of the catalysts. In fact, activities decreased with increasing the amounts of B modification. As known, upon the methanation, the majority of the product is methane. However, considering the selectivity, it can be observed that the selectivity to C_2–C_4 products apparently slightly increased with the B modification. The impact of B modification for the MCM-41 supports on the activities and selectivity is also listed in

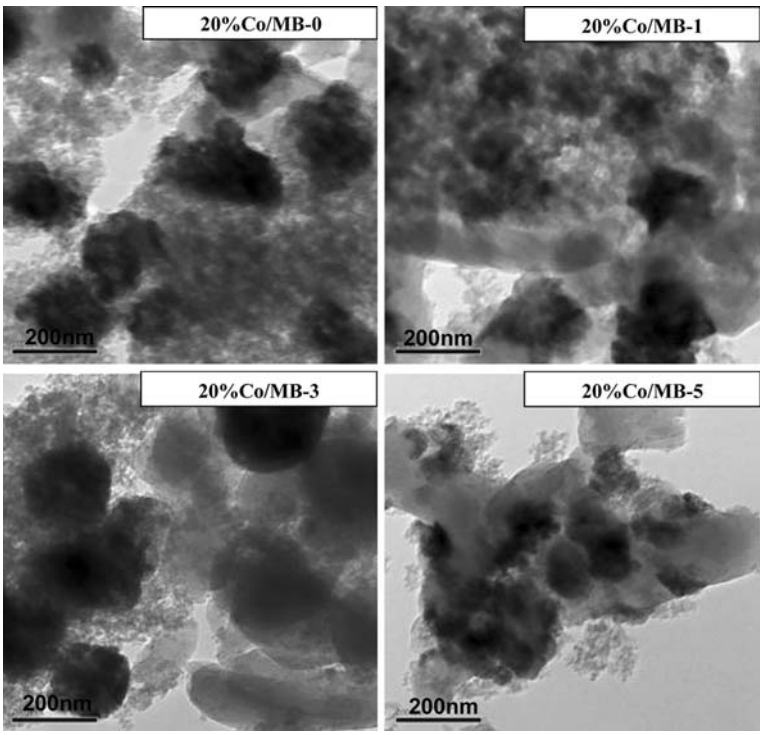

Fig. 10 TEM micrograph for 20-Co/MCM-41 with/without B modification

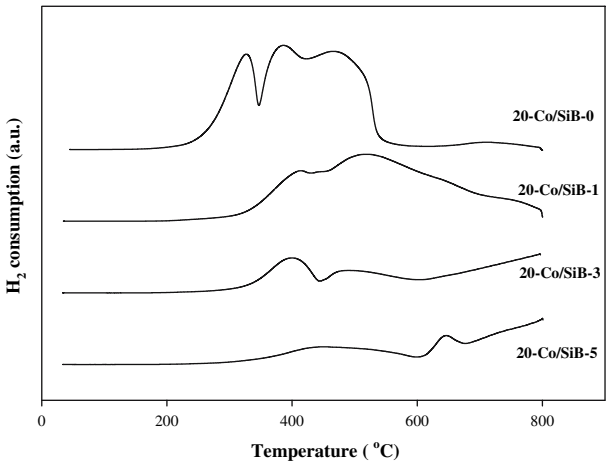

Fig. 11 TPR profiles for 20-Co/SiO_2 with/without B modification

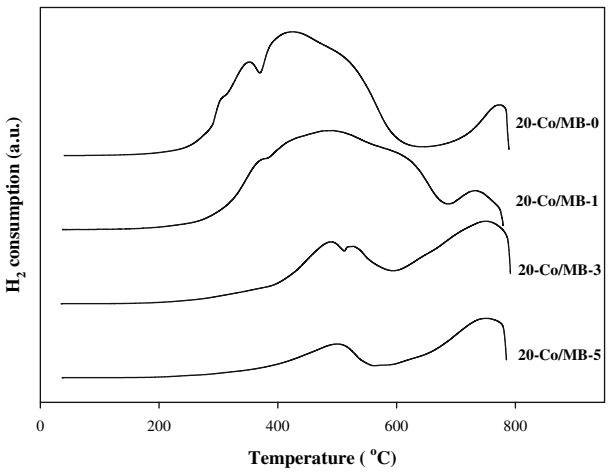

Fig. 12 TPR profiles for 20-Co/MCM-41 with/without B modification

Table 1 as well. Again, as seen from the modification on silica support, activities of Co supported on the MCM-41 essentially decreased with B modification. Even though decreased activities were observed with increased amounts of B modification, the degree of the decreased activities for Co/MB catalysts was less pronounced compared to those from Co/SB catalysts. Besides, the selectivity to C_2–C_4 products obtained from the Co/MB without B and at low loading of B was slightly higher than that from the Co/SB supports. Due to more strong support interaction occurred with the presence of B, it is suggested that the catalysts with B modification would be employed under the liquid phase system in order that the leaching of active species can be prevented. However, it should be noted that the strong support interaction also depends on the nature of active species and supports as well. Here, the interaction between the Co oxide species and silica as well as the MCM-41 supports can be enhanced with the B modification. In order to better understanding different interactions upon various active species and supports, further studies should be investigated.

Table 1 Activities and selectivity of various catalysts during CO hydrogenation

Catalyst sample	Steady-state rate[a] ($\times 10^2$ g CH_2/g cat h)	CH_4 Selectivity (%)	C_2–C_4 Selectivity (%)
20-Co/SiB-0	37.4	99.4	0.6
20-Co/SiB-1	32.7	98.6	1.4
20-Co/SiB-3	14.8	98.2	1.8
20-Co/SiB-5	8.3	98.7	1.3
20-Co/MB-0	37.0	98.3	1.7
20-Co/MB-1	26.2	97.3	2.7
20-Co/MB-3	21.2	98.6	1.4
20-Co/MB-5	18.9	98.7	1.3

[a] CO hydrogenation was carried out at 220 °C, 1 atm and H_2/CO/Ar = 20/2/8. The steady-state was reached after 5 h as reported

4 Conclusions

It appeared that B modification on the silica and MCM-41 supports resulted in decreased activities based on CO hydrogenation. It indicated that the decreased activities were caused by higher degree of interaction between the Co oxide species and the supports with the presence of B resulting in the decreased reducibility. In particular, the impact of B modification on catalytic activities was more pronounced for Co/SB catalysts when increased the amounts of B loading. However, it was found that the selectivity to C_2–C_4 products increased at low B loading, especially for Co/MB catalyst under methanation condition.

Acknowledgments We thank the Thailand Research Fund (TRF) and the graduate school at Chulalongkorn University (90th Anniversary of CU under the Golden Jubilee Fund) for financial support of this project. Guidance of the MCM-41 preparation by Dr. Panpranot is greatly appreciated.

References

1. Withers HP Jr., Eliezer KF, Mitchell JW (1990) Ind Eng Chem Res 29:1807
2. Iglesia E (1997) Appl Catal A 161:59
3. Brady RC, Pettit RJ (1981) J Am Chem Soc 103:1287
4. Panpranot J, Kaewkun S, Praserthdam P, Goodwin JG Jr. (2003) Catal Lett 91:95
5. Panpranot J, Goodwin JG Jr., Sayari A (2002) Catal Today 77:269
6. Kogelbauer A, Weber JC, Goodwin JG Jr. (1995) Catal Lett 34:259
7. Dalai AK, Das TK, Chaudhari KV, Jacobs G, Davis BH (2005) Appl Catal A 289:135
8. Das TK, Conner WA, Li JL, Jacobs G, Dry ME, Davis BH (2005) Energy Fuels 19:1430
9. Jongsomjit B, Panpranot J, Goodwin JG Jr. (2001) J Catal 204:98
10. Jongsomjit B, Goodwin JG Jr. (2002) Catal Today 77:191
11. Jongsomjit B, Panpranot J, Goodwin JG Jr. (2003) J Catal 215:66
12. Jongsomjit B, Sakdamnuson C, Goodwin JG Jr., Praserthdam P (2004) Catal Lett 94:209
13. Jongsomjit B, Sakdamnuson C, Praserthdam P (2005) Mater Chem Phys 89:395
14. Jongsomjit B, Wongsalee T, Praserthdam P (2005) Mater Chem Phys 92:572
15. Jongsomjit B, Wongsalee T, Praserthdam P (2005) Catal Commun 6:705
16. Wongsalee T, Jongsomjit B, Praserthdam P (2006) Catal Lett 108:55
17. Kresge CT, Leonowicz ME, Roth WJ, Vartuli JC, Beck JS (1992) Nature 359:710
18. Beck JS, Varturi JC, Roth WJ, Leonowicz ME, Kresge CT, Schmitt KD, Chu CTW, Olson DH, Sheppard EW, McCullen SB, Higgins JB, Schlenker JL (1992) J Am Chem Soc 114:10834
19. Corma A, Martines V, Soria VJ (1997) J Catal 169:480
20. Song CS, Reddy KM (1999) Appl Catal A 176:1
21. Schuth F, Wingen A, Sauer J (2001) Micropor Mesopor Mater 465:44
22. Panpranot J, Pattamakomsan K, Goodwin JG Jr., Praserthdam P (2004) Catal Commun 5:583
23. Zhang Y, Wei D, Hammache S, Goodwin JG Jr. (1999) J Catal 188:281
24. Schanke D, Vada S, Blekkan EA, Hilmen A, Hoff A, Holmen A (1995) J Catal 156:85
25. Coville NJ, Li J (2002) Catal Today 71:403
26. Li J, Jacobs G, Zhang Y, Das T, Davis BH (2002) Appl Catal A Gen 223:195